ERADication of EDEM1 occurs by selective autophagy and requires deglycosylation by cytoplasmic peptide N-glycanase

Park, Sujin ; Jang, Insook ; Zuber, Christian ; Lee, Yangsin ; Cho, Jin Won ; Matsuo, Ichiro ; Ito, Yukishige ; Roth, Jürgen

Abstract: ER degradation-enhancing -mannosidase-like 1 protein (EDEM1) is involved in the routing of misfolded glycoproteins for degradation in the cytoplasm. Previously, we reported that EDEM1 leaves the endoplasmic reticulum via non-COPII vesicles (Zuber et al. in Proc Natl Acad Sci USA 104:4407-4412, 2007) and becomes degraded by basal autophagy (Le Fourn et al. in Cell Mol Life Sci 66:1434-1445, 2009). However, it is unknown which type of autophagy is involved. Likewise, how EDEM1 is targeted to autophagosomes remains elusive. We now show that EDEM1 is degraded by selective autophagy. It colocalizes with the selective autophagy cargo receptors p62/SQSTM1, neighbor of BRCA1 gene 1 (NBR1) and autophagy-linked FYVE (Alfy) protein, and becomes engulfed by autophagic isolation membranes. The interaction with p62/SQSTM1 and NBR1 is required for routing of EDEM1 to autophagosomes since it can be blocked by short inhibitory RNA knockdown of the cargo receptors. Furthermore, p62/SQSTM1 interacts only with deglycosylated EDEM1 that is also ubiquitinated. The deglycosylation of EDEM1 occurs by the cytosolic peptide N-glycanase and is a prerequisite for interaction and aggregate formation with p62/SQSTM1 as demonstrated by the effect of peptide N-glycanase inhibitors on the formation of protein aggregates. Conversely, aggregation of p62/SQSTM1 and EDEM1 occurs independent of cytoplasmic histone deacetylase. These data provide novel insight into the mechanism of autophagic degradation of the ER-associated protein degradation (ERAD) component EDEM1 and disclose hitherto unknown parallels with the clearance of cytoplasmic aggregates of misfolded proteins by selective autophagy.

DOI: https://doi.org/10.1007/s00418-014-1204-3

Histochem Cell Biol (2014) 142:153–169
DOI 10.1007/s00418-014-1204-3

ORIGINAL PAPER

ERADication of EDEM1 occurs by selective autophagy and requires deglycosylation by cytoplasmic peptide *N*-glycanase

Sujin Park · Insook Jang · Christian Zuber · Yangsin Lee · Jin Won Cho · Ichiro Matsuo · Yukishige Ito · Jürgen Roth

Accepted: 22 February 2014 / Published online: 25 March 2014

Abstract ER degradation-enhancing α-mannosidase-like 1 protein (EDEM1) is involved in the routing of misfolded glycoproteins for degradation in the cytoplasm. Previously, we reported that EDEM1 leaves the endoplasmic reticulum via non-COPII vesicles (Zuber et al. in Proc Natl Acad Sci USA 104:4407–4412, 2007) and becomes degraded by basal autophagy (Le Fourn et al. in Cell Mol Life Sci 66:1434–1445, 2009). However, it is unknown which type of autophagy is involved. Likewise, how EDEM1 is targeted to autophagosomes remains elusive. We now show that EDEM1 is degraded by selective autophagy. It colocalizes with the selective autophagy cargo receptors p62/SQSTM1, neighbor of BRCA1 gene 1 (NBR1) and autophagy-linked FYVE (Alfy) protein, and becomes engulfed by autophagic isolation membranes. The interaction with p62/SQSTM1 and NBR1 is required for routing of EDEM1 to autophagosomes since it can be blocked by short inhibitory RNA knockdown of the cargo receptors. Furthermore, p62/SQSTM1 interacts only with deglycosylated EDEM1 that is also ubiquitinated. The deglycosylation of EDEM1 occurs by the cytosolic peptide *N*-glycanase and is a prerequisite for interaction and aggregate formation with p62/SQSTM1 as demonstrated by the effect of peptide *N*-glycanase inhibitors on the formation of protein aggregates. Conversely, aggregation of p62/SQSTM1 and EDEM1 occurs independent of cytoplasmic histone deacetylase. These data provide novel insight into the mechanism of autophagic degradation of the ER-associated protein degradation (ERAD) component EDEM1 and disclose hitherto unknown parallels with the clearance of cytoplasmic aggregates of misfolded proteins by selective autophagy.

Keywords EDEM1 · Endoplasmic reticulum · Selective autophagy · Cytosolic peptide *N*-glycanase · LC3 · NBR1 · p62/SQSTM1 · Alfy

Abbreviations

Alfy	Autophagy-linked FYVE protein
BODY-$(GlcNAc)_2$-CIAc	Chloroacetamidyl chitobiose coupled to 4,4-difluoro-5,7-dimethyl-4-bora-3a,4a-diaza-*s*-indacene-3-propionic acid
PNGase	Cytoplasmic peptide *N*-glycanase
EDEM1	ER degradation-enhancing α-mannosidase-like 1 protein
ER	Endoplasmic reticulum
ERAD	ER-associated protein degradation

Sujin Park and Insook Jang have contributed equally to this work.

S. Park · I. Jang · Y. Lee · J. W. Cho · J. Roth (✉)
WCU Program, Department of Integrated OMICS for Biomedical Science, Yonsei University Graduate School, Seoul 120-749, Korea
e-mail: jurgen.roth@bluewin.ch

C. Zuber · J. Roth
Division of Cell and Molecular Pathology, Department of Pathology, University of Zurich, 8091 Zurich, Switzerland

I. Matsuo
Department of Chemistry and Chemical Biology, Gunma University, Maebashi, Gunma 376-8515, Japan

Y. Ito
Synthetic Cellular Chemistry Laboratory, RIKEN, Wako, Saitama 351-0198, Japan

Y. Ito
ERATO Glycotrilogy Project, JST, Wako, Saitama 351-0198, Japan

LC3	Microtubule-associated protein 1 light chain 3 beta
man	Mannose
GlcNAc	*N*-Acetylglucosamine
NBR1	Neighbor of BRCA1 gene 1
p62/SQSTM1	Sequestosome 1
siRNA	Short inhibitory RNA
Z-VAD(OMe)-fmk	Carbobenzyloxy-Val-Ala-Asp-α-fluoromethylketone

Introduction

Cellular homeostasis relies on the proper function and cooperation of various networks including protein *N*-glycosylation, protein quality control in the endoplasmic reticulum (ER), ER-associated degradation (ERAD) of glycoproteins, the ubiquitin–proteasome system as well as macroautophagy (referred to here as autophagy) (Araki and Nagata 2012; Eisele et al. 2010; Helenius and Aebi 2004; Mizushima and Komatsu 2011; Roth et al. 2010; Wolf 2011; Wong and Cuervo 2012). Autophagy is an essential, constitutively occurring process through which part of the cytoplasm and organelles are delivered to lysosomes for degradation (Mizushima and Komatsu 2011; Mizushima et al. 2008; Wang and Klionsky 2011). Both at a basal rate and after stimulation by various forms of stress, autophagy is crucial for preserving cellular homeostasis and to prevent cell and tissue damage due to accumulation of protein aggregates or damaged organelles. Likewise, ER protein quality control and ERAD are of fundamental importance for cellular homeostasis by freeing the ER from misfolded glycoproteins or incompletely assembled multisubunit proteins, thereby preventing ER stress, which may lead to cell damage and apoptosis (Araki and Nagata 2012; Braakman and Bulleid 2011; Hutt et al. 2009; Roth et al. 2010; Zuber and Roth 2009).

A functional link exists between protein *N*-glycosylation, ER protein quality control and ERAD since mannose trimming of glycoproteins in the ER has been shown to be fate-determining for misfolded glycoproteins (Helenius and Aebi 2004; Jakob et al. 1998; Roth et al. 2010). The finding that a specific $Man_8GlcNAc_2$ oligosaccharide is involved in targeting misfolded glycoproteins for ERAD (Jakob et al. 1998) led to the discovery of ER degradation-enhancing α-mannosidase-like protein 1 (EDEM1) (Hosokawa et al. 2001; Jakob et al. 2001; Nakatsukasa et al. 2001) and subsequently of OS-9, another ERAD-enhancing protein (Bhamidipati et al. 2005; Buschhorn et al. 2004; Kim et al. 2005; Szathmary et al. 2005). EDEM1 is a α1,2 mannosidase, which trims the $Man_8GlcNAc_2$ oligosaccharides to $Man_7GlcNAc_2$ oligosaccharides (Clerc et al. 2009; Gauss et al. 2011; Hosokawa et al. 2010; Olivari et al. 2006; Quan et al. 2008) that are recognized by OS-9 (Bhamidipati et al. 2005; Hosokawa et al. 2009; Kim et al. 2005; Quan et al. 2008; Szathmary et al. 2005). Hence, the concerted action of EDEM1 and OS-9 is important for the routing of misfolded glycoproteins to the dislocation complex of the ER membrane (Cormier et al. 2009; Denic et al. 2006; Gauss et al. 2006; Quan et al. 2008).

The ERAD machinery component EDEM1 exists as a membrane-bound and a soluble, heterogeneously glycosylated protein (Tamura et al. 2011; Zuber et al. 2007). In contrast to the wide-spread presence in the ER of other ERAD components such as glucosidase II (Lucocq et al. 1986) and UDP-glucose: glycoprotein glucosyltransferase (Zuber et al. 2001), endogenous EDEM1 has a very limited occurrence in the ER as demonstrated by immunocytochemistry and density gradient analysis (Le Fourn et al. 2009; Zuber et al. 2007). By immunogold electron microscopy, most EDEM1 was found in ≥150 nm non-COPII vesicles originating at simple ER cisternae (Zuber et al. 2007) outside the canonical transitional ER exit sites where COPII-coated carriers for ER-to-Golgi transport are formed (Bannykh et al. 1996; Palade 1975). Upon induction of the Ire1α/Xbp1 ER stress response pathway by overexpression of misfolded proteins, EDEM1 and other ERAD components are upregulated to increase the capacity of ERAD (Hosokawa et al. 2001; Olivari et al. 2005). However, when solely overexpressed, EDEM1 is incorrectly present throughout the ER and evokes cytotoxic effects presumably by indiscriminately interacting with mannose-trimmed glycoproteins (Le Fourn et al. 2009). Thus, its limited presence in the ER (Zuber et al. 2007), cytotoxicity when overexpressed (Le Fourn et al. 2009) and adaptive upregulation following an increase in ERAD substrates (Bernasconi et al. 2012; Hosokawa et al. 2001; Olivari et al. 2005) are all indicators of a well-regulated expression of EDEM1, which is important for ERAD tuning (Cali et al. 2008).

We and others previously demonstrated that endogenous EDEM1 is constitutively degraded by autophagy (Cali et al. 2008; Le Fourn et al. 2009) and not by proteasomes (Le Fourn et al. 2009). Furthermore, we observed that the deglycosylated EDEM1 preferentially exists as Triton X-100 insoluble aggregates that are removed by autophagy (Le Fourn et al. 2009). However, the molecular mechanism involved in targeting EDEM1 for autophagy and the type of autophagy implicated, either non-selective or selective, are currently not known.

In the present study, we show that autophagy of EDEM1 in HepG2 cells depends on its interaction with selective autophagy cargo receptors since knockdown of p62/SQSTM1 and NBR1 blocked routing of EDEM1 to autophagosomes. Furthermore, we found that deglycosylation of EDEM1 by the cytosolic peptide *N*-glycanase (PNGase) is required for the interaction with the cargo

receptor p62/SQSTM1 and is a prerequisite for aggregate formation with p62/SQSTM1. Notably, the deglycosylated EDEM1, but not its glycosylated form, appears to be ubiquitinated, providing a basis for binding of cargo receptors. Thus, our findings provide new insight into the degradation pathway of the ERAD component EDEM1 by selective autophagy.

Materials and methods

Reagents

BODY-$(GlcNAc)_2$-CIAc (chloroacetamidyl chitobiose coupled to 4,4-difluoro-5,7-dimethyl-4-bora-3a,4a-diaza-*s*-indacene-3-propionic acid) was synthesized as described (Hagihara et al. 2007) and Z-VAD(OMe)-fmk (carbobenzyloxy-Val-Ala-Asp-α-fluoromethylketone) was purchased from Bachem (N-1560). Diaminobenzidine tetrahydrochloride (D5905, DAB), wortmannin (w1628), trichostatin A (T8552-1MG), sodium deoxycholate (D6750) and saponin (S4521) were from Sigma-Aldrich (St. Louis, MO, USA), glutaraldehyde (354400) and osmium tetroxide (OX0260) from EMD (Gibbstown, NJ, USA), paraformaldehyde from Merck (Basel, Switzerland, 818715), protease inhibitor cocktail from Roche Applied Science (Basel, Switzerland, 78430) and Epon-Araldite kits from Fluka (Buchs, Switzerland, 45345). All other chemicals were of p.a. grade and from Sigma-Aldrich.

The following anti-EDEM1 antibodies were used: affinity-purified rabbit polyclonal antibodies against C terminal 15 amino acids of human EDEM1 (Zuber et al. 2007) and against a C-terminal 50 amino acid peptide (Aviva Systems Biology, San Diego, CA, USA, ARP47054-P050,), affinity-purified rabbit polyclonal anti-peptide antibody (Sigma, E8406) and goat antibody against a C-terminal peptide (Santa Cruz Biotechnology, Santa Cruz, CA, USA, sc-27391, C-19). Mouse monoclonal antibodies against LC3 (152-3) were from MBL International, mouse monoclonal anti-NBR1 (H00004077) and rabbit polyclonal anti-Alfy (NBP1-06006) were from Novus Biologicals (Littletown, CO, USA) and guinea pig polyclonal antibodies against a C-terminal peptide of human p62/SQSTM1 (GP62-C) from PROGEN (Heidelberg, Germany). Mouse monoclonal anti-mono- and polyubiquitin antibody was from Enzo Life Sciences (Dong In Biotech Co., Ltd., Seoul; BML-PW8810) and rabbit anti-β-actin antibody from Cell Signaling Technology, Inc. (Danvers, MA, USA; 4967S).

Horseradish peroxidase-conjugated $(Fab)_2$ goat anti-rabbit IgG antibodies (111-005-006) were purchased from Jackson Immunoresearch Laboratories, Inc. (West Grove, PA, USA) and horseradish peroxidase-conjugated goat anti-mouse IgG (sc-3738), goat anti-rabbit IgG (sc-3739), donkey anti-goat IgG (sc-3743) and goat anti-guinea pig IgG (sc-3732) were from Santa Cruz Biotechnology. DyLight488-conjugated affinity-purified $F(ab)_2$ fragments of donkey anti-goat IgG (705-546-147), rhodamine Red-X-conjugated affinity-purified donkey anti-rabbit IgG (711-296-152), Cy2-conjugated affinity-purified donkey anti-guinea pig IgG (706-225-148), Cy2-conjugated affinity-purified $F(ab)_2$ fragments of donkey anti-mouse IgG (715-226-020), and AMCA-conjugated affinity-purified $F(ab)_2$ fragments of donkey anti-guinea pig IgG (706-156-148) as well as 12-nm gold-labeled affinity-pure donkey anti-rabbit IgG (711-205-152) and donkey anti-goat IgG (703-205-155) and 6-nm gold-labeled affinity-pure donkey anti-guinea pig IgG (706-195-148), donkey anti-mouse IgG (715-195-150) and donkey anti-rabbit IgG (711-195-152) were from Jackson Immunoresearch Laboratories, Inc. and Alexa 488 donkey anti-rabbit IgG from Molecular Probes-Invitrogen (Carlsbad, CA, USA, A-21206). Protein A-gold complexes were prepared according to standard protocol (Roth 1982; Roth et al. 1978).

Cell culture

Human HepG2 cells were obtained from ATCC (Manassas, VA, USA) and cultured in complete culture medium (Gibco, Auckland, NZ, 11095-072) supplemented with 10 % fetal bovine serum (Gibco, 10082-139) and 1.0 mM sodium pyruvate. Cell cultures were replenished with fresh medium 16 h before experiments or processing for microscopy. In starvation experiments, cells were grown in serum-free medium for 1.5 h.

Inhibitor treatment

To inhibit PNGase, HepG2 cells were treated either with BODY-$(GlcNAc)_2$-CIAc (20 μM, 2 h) or Z-VAD(OMe)-fmk (50 μM, 3 h). For Western blot, cells were lysed in SDS-PAGE sample buffer and processed as detailed below. For immunofluorescence, cells grown on coverslips were treated either with BODY-$(GlcNAc)_2$-CIAc alone or in combination with wortmannin (50 nM, 4 h) and processed for immunofluorescence (see below). For inhibition of autophagy, cells were treated with wortmannin (50 nM) and for inhibition of histone deacetylases with trichostatin A (10 mM) alone and in combination with wortmannin.

siRNA

p62/SQSTM1 siRNA was purchased from Santa Cruz Biotechnology (human, sc-29679). For NBR1 knockdown, sense 5′-GAG AAC AAG UGG UUA ACG A-3′ and antisense 5′-UCG UUA ACC ACU UGU UCU C-3′ were used (Larsen et al. 2010). As control, MISSION®

siRNA universal negative control #1 (Sigma, SIC001) was used. HepG2 cells at about 40 % confluence were transfected using Lipofectamine® RNAiMAX (Invitrogen, 13778-075) following the supplier's instructions. Cells were analyzed by immunofluorescence and Western blotting after 48 h.

Confocal immunofluorescence microscopy

Cells were grown on precision coverslips (0.17 ± 0.01 mm thickness; Glaswarenfabrik Karl Hecht GmbH & Co KG, Sondheim, Germany) and fixed in 3 % formaldehyde (freshly prepared from paraformaldehyde) in PBS for 30 min at 37 °C. Free aldehyde groups were quenched with 50 mM NH_4Cl 30 min on ice (Roth et al. 1989), and cells were permeabilized with saponin (0.3 %, 10 min) as described (Zuber et al. 2000, 2007).

For single and double immunofluorescence, rabbit or goat anti-human EDEM1 antibodies (1:100), guinea pig anti-human p62/SQSTM1 antibodies (1:100), mouse monoclonal anti-NBR1 antibodies (1:50), rabbit polyclonal anti-Alfy antibodies (1:100) and mouse monoclonal anti-LC3 antibodies (1:100) were applied for 2 h followed by rinses (2 × 5 min) in PBS containing 1 % bovine serum albumin and incubation with appropriate fluorescent secondary antibodies for 1 h. DAPI was used for staining of nuclei. After rinses, coverslips were mounted on glass slides with Mowiol.

Immunofluorescence was recorded with a Zeiss LSM 510 confocal microscope (Zeiss, Jena, Germany) using a Plan-Apochromat 100 × objective (1.4 N.A.), and top-to-bottom Z-stacks of optical sections (nominal thickness 200 nm) were generated. In multiple immunofluorescence overlays, effects of *z*-axis pixel shifts were corrected. Colocalization channels were calculated using Meta Imaging Series® MetaMorph software (Meta Series Software 7.7.0; Molecular Devices) and appear in white in all figures. Quantification of single immunofluorescence and of colocalization channels of z-stacks was performed using Meta Imaging Series® MetaMorph software. At least 50 cells from at least three independent experiments were analyzed, and the results are given as the mean ± SE. Illustrations were generated using Photoshop CS3 (version 10.0.1, Adobe Systems, Inc.). When used, linear adjustment of contrast and brightness was applied to the entire composite pictures equally.

Immunoelectron microscopy

HepG2 cells grown to near confluence were fixed in a mixture of 2 % formaldehyde (freshly prepared from paraformaldehyde) and 0.1 % glutaraldehyde (vacuum-distilled) in 0.1 M cacodylate buffer (pH 7.2) for 30 min at initially 37 °C, rinsed with buffer, enclosed in 15 % gelatin, infiltrated stepwise with 0.6, 1.2 and 2.3 M sucrose and frozen in liquid nitrogen. Frozen ultrathin sections were prepared at −110 °C according to Tokuyasu (1989). Before antibody incubations, sections attached to nickel grids were incubated with 2 % gelatine in PBS at 40 °C for 20 min, rinsed with PBS followed by amidation of aldehyde groups with 50 mM NH_4Cl for 30 min on ice (Roth et al. 1989). Ultrathin frozen sections were incubated with rabbit anti-EDEM1 antibodies (1:50) diluted in PBS containing 1 % BSA and 0.01 % Tween 20 for 2 h followed by several rinses in PBS and 8-nm protein A-gold (Roth 1989; Roth et al. 1978) diluted to an absorbance of 0.1 at 520 nm in PBS containing 1 % bovine serum albumin (or 0.2 % skimmed milk) and 0.01 % Tween 20 for 1 h. After rinses in PBS and finally one rinse in distilled water, sections were postfixed with 1 % glutaraldehyde for 5 min and embedded in 2 % methylcellulose containing 0.3 % uranyl acetate.

For double immunogold labeling, ultrathin frozen sections were simultaneously incubated with either rabbit or goat anti-EDEM1 antibodies and antibodies against p62 (1:25), NBR1 (1:5) or Alfy (1:5) for 2 h, washed with buffer and incubated simultaneously with 12-nm gold-labeled goat anti-rabbit IgG or donkey anti-goat IgG (diluted to an absorbance of 0.1 at 520 nm) and either 6-nm gold-labeled goat anti-guinea pig IgG, goat anti-mouse IgG and donkey anti-rabbit IgG (each diluted to an absorbance of 0.065 at 520 nm) for 1 h followed by rinses, postfixation and methylcellulose/uranyl acetate embedding as described above. Specificity of immunogold labeling was assessed as described (Le Fourn et al. 2009; Zuber et al. 2007).

For preembedding immunoperoxidase labeling, cells were grown on coverslips, fixed in situ with 3 % formaldehyde (see above) and permeabilized with 0.05 % saponin followed by incubation with EDEM1 antibodies. After rinses with PBS and incubation with horseradish peroxidase-conjugated $(Fab)_2$ goatanti-rabbit IgG (4 μg/ml in 1 % BSA-PBS), a modified diaminobenzidine reaction was performed as described (Zuber et al. 2007). In controls, EDEM1 antibody was replaced by unrelated antibody (anti-pancreatic amylase) or incubation was performed only with secondary antibody. Serial ultrathin sections from Epon-Araldite-embedded cells were prepared in the plane of the cell monolayer. Sections were observed in a Zeiss 912AB or a Hitachi H-7650 electron microscope at 80 kV, and pictures were taken with 70-mm film sheets or an 11-megapixel CCD XR611-M digital camera (Advanced Microscopy Techniques, Woburn, MA, USA). Pictures were generated using Photoshop CS3 (Adobe Systems, Inc.), and linear adjustment of contrast and brightness was applied.

Immunoprecipitation and Western blot

HepG2 cells were washed twice in cold PBS, mechanically removed and lysed in PBS containing 1 % Triton X-100 and protease inhibitor cocktail. After 30 min incubation on ice, cells were centrifuged at 10,000×*g* for 10 min. The supernatant containing Triton X-100 soluble proteins and the pellet containing Triton X-100 insoluble proteins were washed in cold PBS. The pellet was dissolved by sonication in Laemmli buffer containing 8 M urea, and the urea was diluted out immediately before the start of the immunoprecipitation.

For immunoprecipitation of EDEM1, samples from the Triton X-100 soluble and insoluble materials were sequentially incubated overnight at 4 °C with protein A-Dynal magnetic beads (Invitrogen, Dynal AS, Oslo, Norway) coated with goat anti-EDEM1 followed by beads coated with rabbit anti-EDEM1. Likewise, immunoprecipitates were prepared with beads coated with guinea pig p62 antibodies. Afterward, immunocomplexes were washed four times in PBS containing 1 % Triton X-100, boiled for 8 min and electrophoretically resolved in 8 % polyacrylamide gels and transferred to nitrocellulose. Nitrocellulose membranes were conditioned for 45 min in 5 % skimmed milk in TBS-Tween (20 mM Tris–HCl, pH 7.4, 0.5 M NaCl, 0.1 % Tween 20), incubated overnight at 4 °C with EDEM1, p62 or ubiquitin antibodies, rinsed and incubated for 1 h with the appropriate horseradish peroxidase-conjugated secondary antibodies. Immunoreactive bands were visualized by ECL system (GE Healthcare) and quantified using ImageQuant TL software (GE Healthcare, Bio-Science). β-actin was used for calibration.

For Western blot, cells were harvested and lysed in PBS containing 1 % Triton X-100 and protease inhibitor cocktail. After 30 min incubation on ice, cells were centrifuged at 10,000×*g* for 10 min. The supernatant containing Triton X-100 soluble proteins and the pellet containing Triton X-100 insoluble proteins were washed in cold PBS. The pellet was dissolved by sonication in Laemmli buffer containing 8 M urea. Samples were boiled for 8 min, loaded and resolved by SDS-PAGE and transferred to nitrocellulose membranes, which were incubated with EDEM1 antibodies as described above.

Results

EDEM1 is targeted by selective autophagy cargo receptors and routed to autophagosomes

Previous work with autophagy-defective mouse embryonic fibroblasts (Cali et al. 2008) and human hepatoma HepG2 cells (Le Fourn et al. 2009) has shown the involvement of autophagy in the constitutive degradation of EDEM1. As revealed by confocal immunofluorescence microscopy, EDEM1 puncta in resting HepG2 cells range in size from 0.027 to 0.4 μm^2 (Fig. 1a). When their relation with the autophagosome marker LC3 (Kabeya et al. 2000) was analyzed, EDEM1 puncta of 0.13–0.4 μm^2 size were colocalized with LC3 puncta, whereas smaller EDEM1 puncta (between 0.027 and 0.13 μm^2) were not (Fig. 1a–c). The smaller EDEM1 puncta probably correspond to the EDEM1 vesicles previously identified by immunoelectron microscopy (Zuber et al. 2007). It is well established that autophagy can be stimulated by starvation (Mizushima et al. 2011). Starvation of HepG2 cells greatly increased the number of LC3 puncta (Fig. 1e). The number of EDEM1 puncta was also increased (Fig. 1d) since EDEM1 is upregulated by various forms of cellular stress (Hosokawa et al. 2001; Olivari et al. 2005). As in resting cells, in starved cells, large puncta (between 0.13 and 0.4 μm^2) of EDEM1 and LC3 colocalized, but not the smaller (between 0.027 and 0.13 μm^2) EDEM1 puncta (Fig. 1d–f). This observation provides additional evidence for the presence of EDEM1 in autophagosomes.

Autophagy can either be a non-selective or a selective process (Johansen and Lamark 2011), but it is unknown which one operates in the degradation of EDEM1. Selective autophagy involves various cargo receptors such as p62/SQSTM1 (Bjorkoy et al. 2005), neighbor of BRCA1 gene 1 (NBR1) (Kirkin et al. 2009) and autophagy-linked FYVE protein (Alfy) (Filimonenko et al. 2010; Simonsen et al. 2004). Given this well-established pathway, we first analyzed the relation of EDEM1 with selective autophagy cargo receptors by immunocytochemistry. In resting HepG2 cells, 48.29 % of EDEM1 puncta were colocalized with p62/SQSTM1 puncta (Fig. 1g–i). Previously, we have applied siRNA knockdown of Atg's (Le Fourn et al. 2009) to biochemically demonstrate that EDEM1 is degraded by autophagy. In order to uniformly inhibit autophagy in the cultured cells, we used wortmannin, a selective and potent inhibitor of phosphatidylinositol 3-kinase that inhibits formation of autophagosomes at nanomolar concentrations (Mizushima et al. 2010; Petiot et al. 2000; Powis et al. 1994; Wipf and Halter 2005; Wu et al. 2010). When HepG2 cells were treated with 50 nM wortmannin for 4 h, the total number of EDEM1 puncta increased 5.5-fold (Fig. 1g, j, m) and that of large size (≥0.13 μm^2) puncta 8.8-fold (Fig. 1n). The number of p62/SQSTM1 puncta was also increased (Fig. 1h, k). Total colocalized EDEM1–p62/SQSTM1 puncta were increased 5.2-fold (Fig. 1i, l, o) and colocalized large size (≥0.13 μm^2) puncta a striking 10.3-fold (Fig. 1p). By double immunogold labeling, cytoplasmic single and double labeling for EDEM1 and p62/SQSTM1 was detected in resting (Fig. 2a–c) and wortmannin-treated cells (Fig. 2d–f). As we previously reported

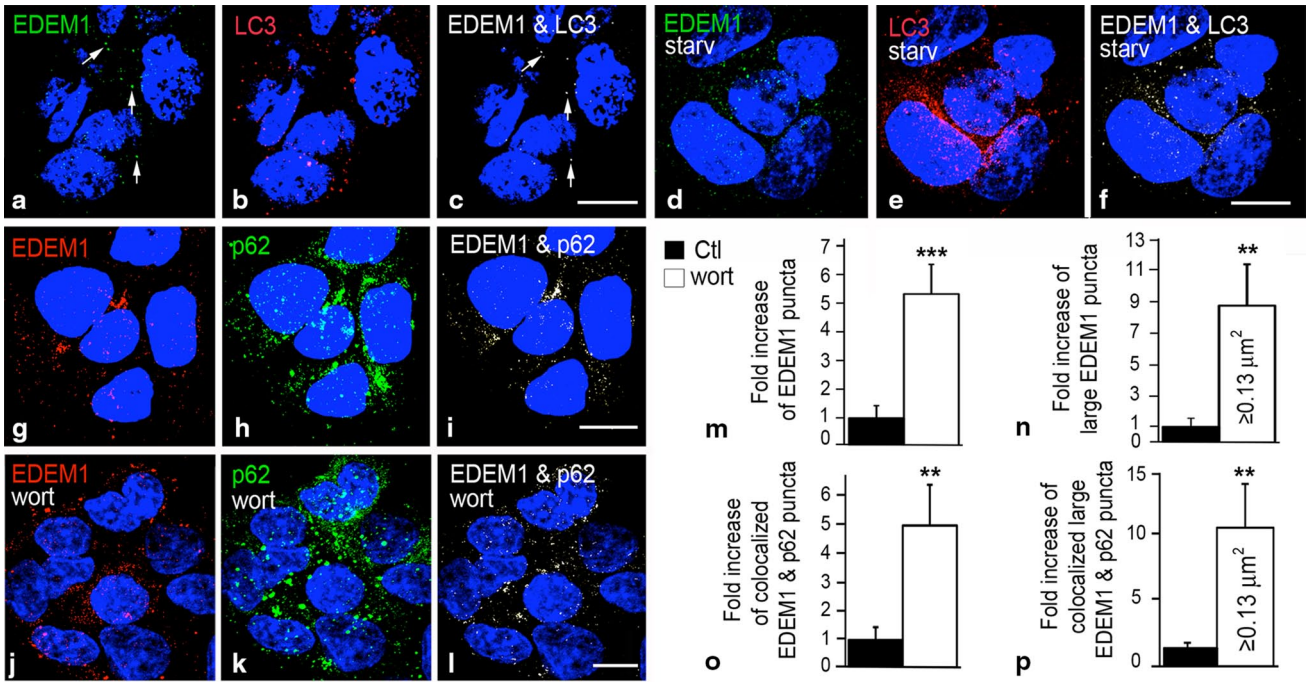

Fig. 1 EDEM1 colocalizes with autophagosomes and the selective autophagy cargo receptor p62/SQSTM1. Confocal analysis of endogenous EDEM1 (**a**) and endogenous LC3 (**b**) demonstrates colocalization of large EDEM1 puncta with autophagosomes (*arrows* in **a**, **c**). Small EDEM1 puncta do not colocalize with LC3 puncta. Colocalization channels appear as white puncta. Starvation increases puncta of EDEM1 (**d**) and LC3 (**e**) and colocalization of EDEM1 and LC3 in large puncta (**f**). Confocal analysis of endogenous EDEM1 (**g**, **j**) and endogenous p62/SQSTM1 (**h**, **k**) shows their colocalization in control (**i**) and wortmannin (wort)-treated cells (**l**). Confocal *top*-to-*bottom* *z*-stacks. *Bars* 10 µm. Quantification of all and of large (≥0.13 µm^2) EDEM1 puncta in control and wortmannin (wort)-treated cells (**m**, **n**). Quantification of all and of large EDEM1 (≥0.13 µm^2) puncta colocalized with p62/SQSTM1 puncta in control and wortmannin (wort)-treated cells (**o**, **p**). $^{**}p < 0.01$; $^{***}p < 0.005$

(Le Fourn et al. 2009), EDEM1 becomes engulfed by isolation membranes as shown by immunoperoxidase electron microscopy (Fig. 2g).

Next, we analyzed the relation between EDEM1 and the cargo receptors NBR1 and Alfy. By double confocal immunofluorescence, 27.25 % of EDEM1 puncta were colocalized with NBR1 puncta (Fig. 3a–c). Following wortmannin treatment, EDEM1 and NBR1 puncta were increased 2.38- and 2.46-fold, respectively (Fig. 3d–g). Colocalized EDEM1 and NBR1 puncta were increased 6.15-fold (Fig. 3f, g). Colocalization of EDEM1 and NBR1 was directly demonstrated by high-resolution double-label immunogold electron microscopy (Fig. 4). Similar observations were made for the colocalization of EDEM1 and Alfy in resting (Fig. 5a–c) and in wortmannin-treated cells (Fig. 5d–f). Colocalization of EDEM1 and Alfy was directly shown by double-label immunogold electron microscopy (Fig. 5g, h). Furthermore, clusters immunoreactive for both EDEM1 and Alfy engulfed by double-membrane structures were observed, which represent bona fide isolation membranes (Fig. 5i). Together, these observations indicate that EDEM1 and the selective autophagy cargo receptors p62/SQSTM1, NBR1 and Alfy are present together in cytoplasmic clusters.

To obtain information about a possible role of p62/SQSTM1 and NBR1 in routing EDEM1 to autophagosomes, siRNA interference was applied. As verified by Western blotting and confocal immunofluorescence, p62/SQSTM1 (Fig. 6a–h) and NBR1 (Fig. 3h–l) could be efficiently knocked down. Although the cargo receptor knockdown resulted in a significantly increased amount of EDEM1 (Figs. 3h, 6i), colocalization of EDEM1 and p62/SQSTM1 (Fig. 6b–h) or NBR1 (Fig. 3i–l) was significantly decreased. Of note, the siRNA knockdown of p62/SQSTM1 and NBR1 had no significant influence on the number of LC3 puncta (Figs. 3n, q, s, 6k, n, p), an established marker for autophagosomes (Kabeya et al. 2000). However, and strikingly, the siRNA-mediated knockdown of p62/SQSTM1 and NBR1 resulted in a significant reduction in colocalization of EDEM1 and LC3 (Figs. 3o, r, s, 6l, o, p). Together, this indicates a requirement of p62/SQSTM1 and NBR1 for routing of EDEM1 to autophagosomes.

The codistribution of EDEM1 with p62/SQSTM1, NBR1 and Alfy is unanticipated since the selective autophagy cargo receptors are cytosolic proteins. We have previously shown by immunoelectron microscopy and

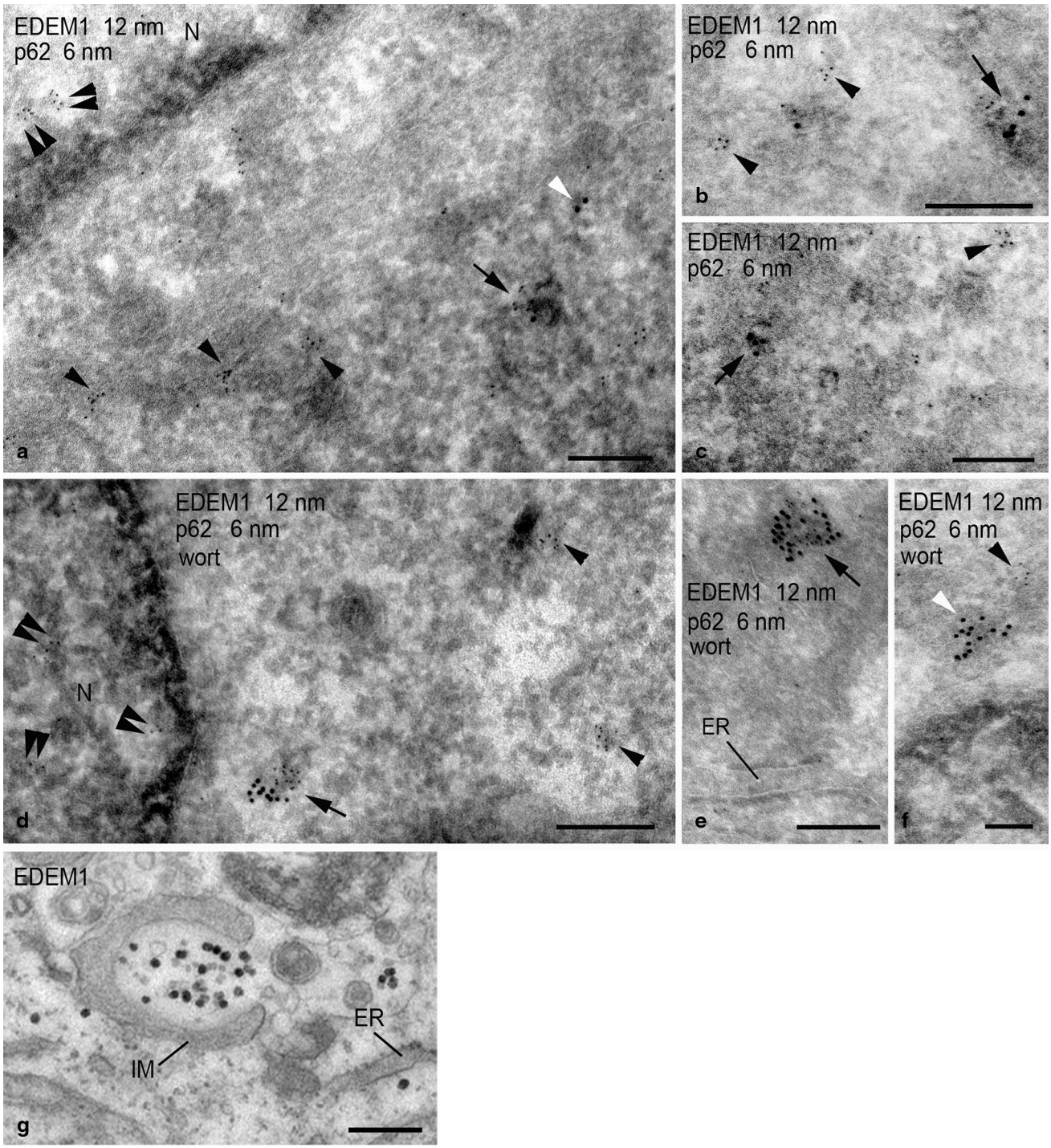

Fig. 2 EDEM1 and p62/SQSTM1 colocalize in the cytoplasm. Double immunogold labeling of ultrathin frozen sections of control (**a**–**c**) and wortmannin (wort)-treated (**d**–**f**) HepG2 cells demonstrates colocalization of EDEM1 (12-nm gold particles) and p62/SQSTM1 (6-nm gold particles) in clusters lacking a membrane (*arrows* in **a**–**e**). *White arrowheads*: single EDEM1 labeling, *black arrowheads*: single p62/SQSTM1 labeling. p62/SQSTM1 is also detected in the nucleus (*double arrowheads* in **a**, **d**) since it contains NLS and NES (Pankiv et al. 2010). EDEM1 is engulfed by an isolation membrane (IM in **g**), preembedding immunoperoxidase labeling. *N* nucleus, *ER* endoplasmic reticulum. *Bars* 200 nm (**a**–**d**), 250 nm (**e**), 100 nm (**f**), 500 nm (**g**)

serial thin section analysis that EDEM1 exits the ER in ≥150 nm non-COPII-coated vesicles (Zuber et al. 2007). However, as shown here by immunogold labeling, EDEM1 additionally exists in non-membrane-limited clusters with p62/SQSTM1 (Fig. 2a–f), NBR1 (Fig. 4a–e) or Alfy (Fig. 5g–i).

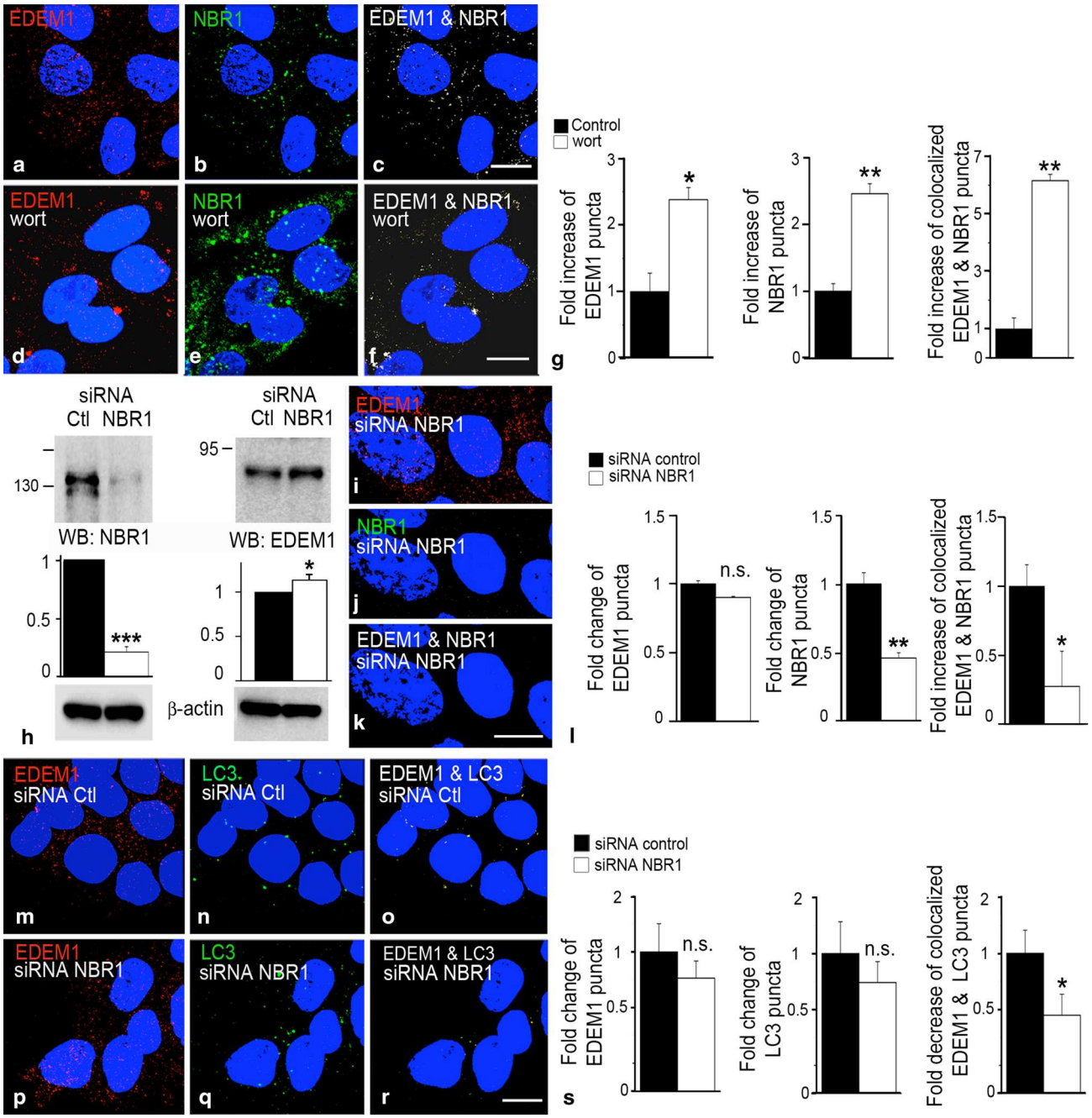

Fig. 3 EDEM1 colocalizes with selective autophagy cargo receptor NBR1, and knockdown of NBR1 impedes the colocalization of EDEM1 and LC3. Confocal *top*-to-*bottom* *z*-stacks illustrating the distribution of endogenous EDEM1 (**a**) and endogenous NBR1 (**b**) and their colocalization (**c**). *Bar* 10 μm. Confocal *top*-to-*bottom* *z*-stacks demonstrating the effect of autophagy inhibition by wortmannin (wort) on endogenous EDEM1 (**d**) NBR1 (**e**) and their colocalization (**f**). *Bar* 10 μm. **g** Quantification of EDEM1 puncta (*left panel*), NBR1 puncta (*middle panel)* and their colocalization (*right panel*) in control and wortmannin (wort)-treated cells. **h** Western blot showing the effect of siRNA silencing on NBR1 (*left panel*) and on EDEM1 protein levels (*right panel*). **i–k** Confocal *top*-to-*bottom* *z*-stacks illustrating the effect of NBR1 siRNA knockdown on EDEM1 puncta (**i**), NBR1 puncta (**j**) and colocalized EDEM1-NBR1 puncta (**k**). *Bar* 10 μm. **l** Quantification of NBR1 siRNA knockdown effect on EDEM1 puncta (*left panel*) NBR1 puncta (*middle panel)* and their colocalization (*right panel*). **m–r** Confocal *top*-to-*bottom* *z*-stacks depicting the effect of NBR1 siRNA knockdown on EDEM1 (**m**, **p**) and LC3 (**n**, **q**) puncta and their colocalization (**o**, **r**). *Bar* 10 μm. **s** Quantification of EDEM1 puncta (*left panel*), LC3 puncta (*middle panel*) and colocalized EDEM1 and LC3 puncta (*right panel*) following NBR1 siRNA knockdown. $*p < 0.05$; $**p < 0.01$; $***p < 0.005$

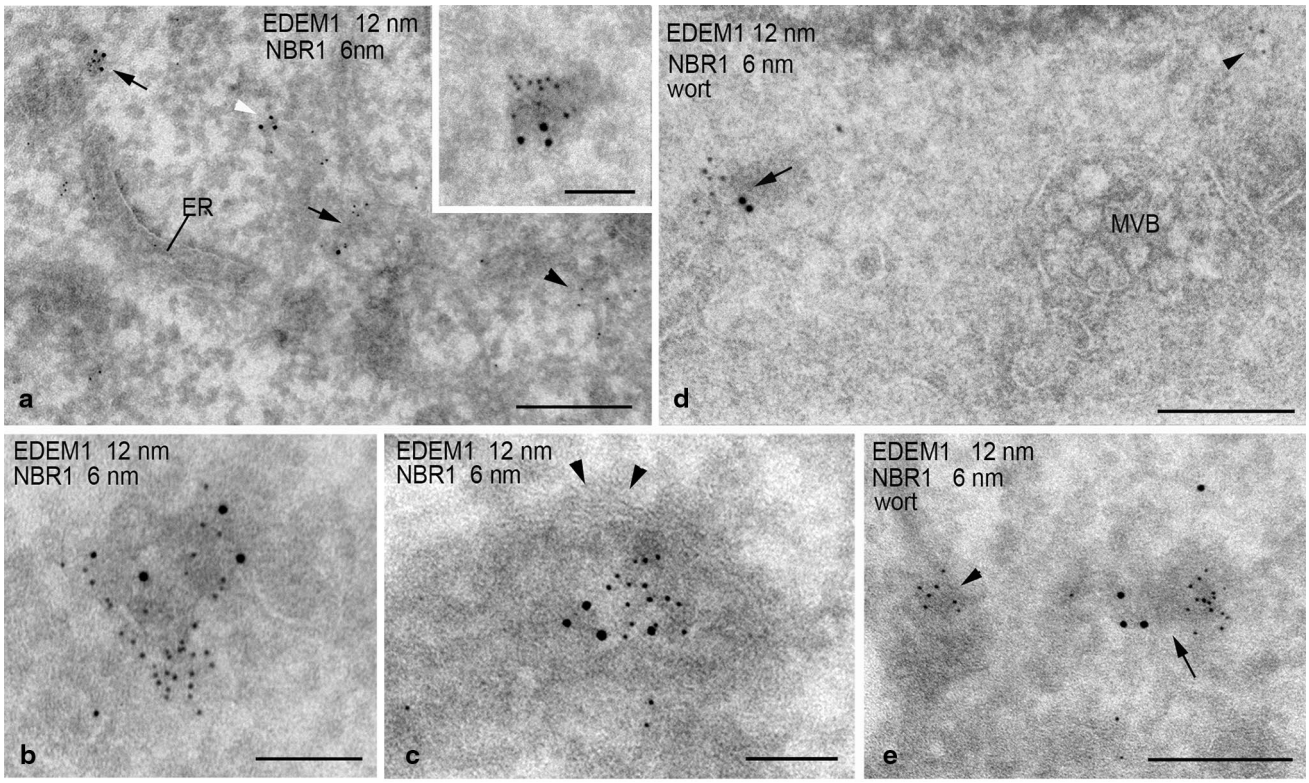

Fig. 4 EDEM1 and NBR1 colocalize in the cytoplasm and become engulfed by isolation membranes. Double immunogold labeling of ultrathin frozen sections for EDEM1 (12-nm gold particles) and NBR1 (6-nm gold particles) in control (**a**–**c**) and wortmannin (wort)-treated cells (**d**, **e**). *Arrows* clusters of EDEM1–NBR1 double labeling; *white arrowheads*: single EDEM1 labeling; *black arrowheads*: single NBR1 labeling. **c** A cytoplasmic EDEM1–NBR1 cluster is partially encircled by an isolation membrane (*arrowheads*). *ER* endoplasmic reticulum. *Bars* 200 nm (**a**, **d**, **e**); 100 nm (**b**, **c**, inset of **a**)

Inhibition of histone deacetylase does not prevent clustering of EDEM1–p62/SQSTM1 complexes

The large puncta containing EDEM1 and p62/SQSTM1, NBR1 or Alfy in control and wortmannin-treated cells are scattered throughout the cytoplasm (Figs. 1c, i, l, 3c, f, 5c, f). This is in contrast to the pericentrosomal location of aggresomes and other types of cytoplasmic inclusion bodies composed of ubiquitinated misfolded proteins and p62/SQSTM1 (Hirano et al. 2009; Johnston et al. 1998; Zatloukal et al. 2002). The formation of aggresomes (Kawaguchi et al. 2003) and their clearance by autophagy (Iwata et al. 2005; Lee et al. 2010) depends on microtubules and the histone deacetylase-6-dynein transport system.

When HepG2 cells were treated with wortmannin to enhance formation of EDEM1–p62/SQSTM1 clusters through inhibition of autophagy, and simultaneously with trichostatin A, a broad-spectrum inhibitor of histone deacetylases (Furumai et al. 2001), there was no effect on the formation of wortmannin-induced large puncta containing EDEM1 and p62/SQSTM1 (Fig. 7). This indicates a stochastic process in the formation of this type of protein aggregate. Previous immunofluorescence results (Bjorkoy et al. 2005; Pankiv et al. 2007), and the results of the present immunogold electron microscopy analysis also show that p62/SQSTM1 bodies (Fig. 2) as well as aggregates of EDEM1 with NBR1 (Fig. 4) and Alfy (Fig. 5g–i) are distinct from aggresomes. They not only differ in size and subcellular distribution, but also by the absence of a cage of intermediate filaments, which surrounds aggresomes. Notably, p62/SQSTM1 bodies not only exist in stressed cells (Clausen et al. 2010; Pankiv et al. 2007; Szeto et al. 2006) but as shown here also in resting cells where they can represent an intermediate in the constitutive degradation of EDEM1 by selective autophagy. In more general terms, this shows that in mammalian cells, as in yeast (Chen et al. 2012; Kaganovich et al. 2008), different types of cytoplasmic protein aggregates exist, which are targeted either by autophagy or by proteasomes.

Deglycosylation of EDEM1 by cytosolic peptide *N*-glycanase is important for its interaction with p62/SQSTM1

Our previous work on HepG2 cells has shown that EDEM1 exists mainly as an Endo H-sensitive and Triton X-100

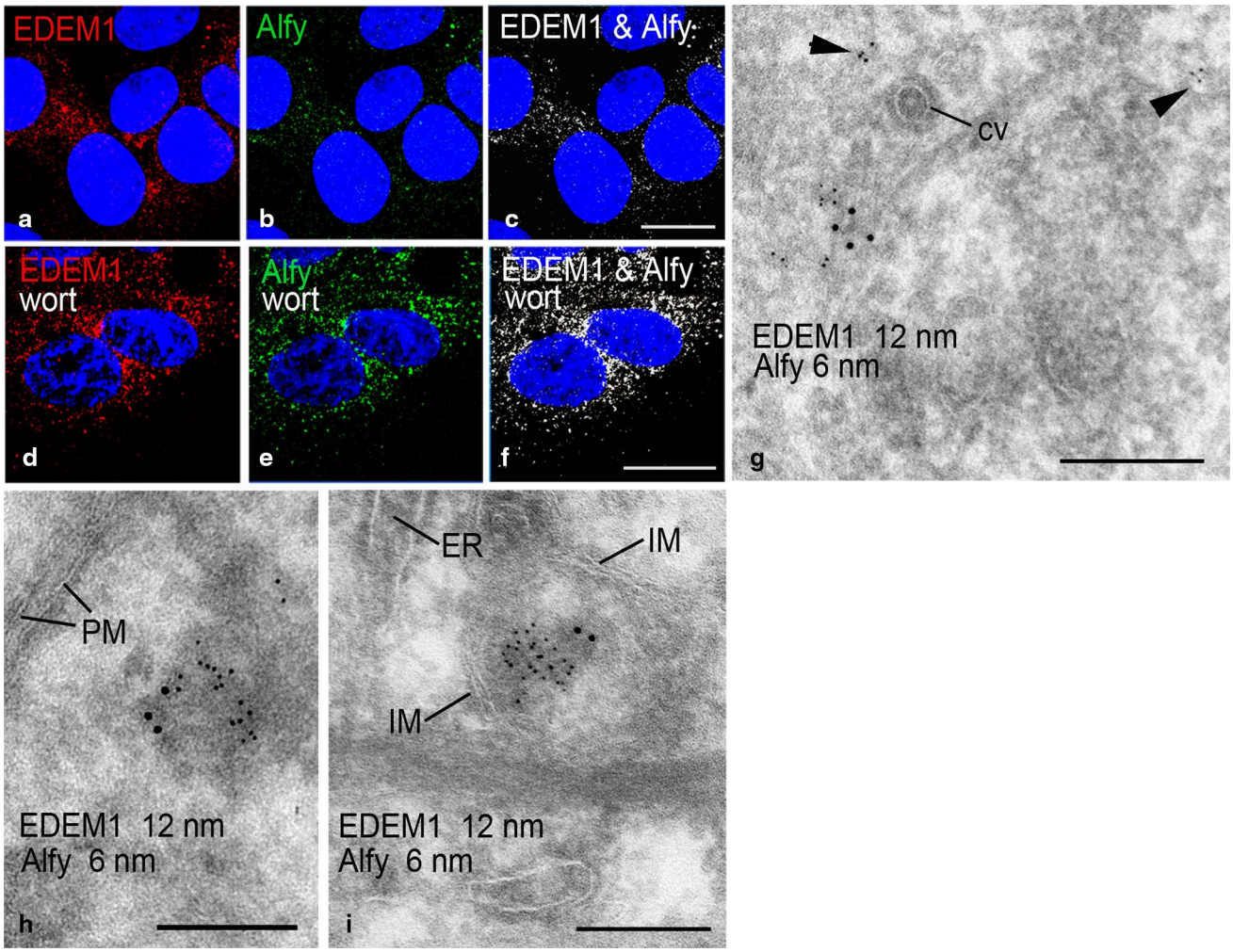

Fig. 5 EDEM1 colocalizes with the selective autophagy cargo receptor Alfy and becomes engulfed by isolation membranes. **a–c** Confocal *top*-to-*bottom* *z*-stacks showing the distribution of endogenous EDEM1 (**a**) and endogenous Alfy (**b**) and their colocalization (**c**). **d–f** Wortmannin (wort) treatment to inhibit autophagy increases EDEM1 puncta (**d**) and Alfy puncta (**e**) and their colocalization (**f**). *Bars* 10 μm. **g–i** Double immunogold labeling of ultrathin frozen sections for EDEM1 (12-nm gold particles) and Alfy (6-nm gold particles) in control HepG2 cells shows their colocalization in not membrane-limited clusters in the cytoplasm and engulfment by isolation membrane (IM in **i**). *Arrowheads* in **g** indicate single Alfy labeling. *ER* endoplasmic reticulum, *PM* plasma membrane, *cv* coated vesicle. *Bars* 200 nm (**g–i**)

soluble form and in much lesser amounts in a deglycosylated form (Zuber et al. 2007). Further analysis revealed that the deglycosylated EDEM1 is present almost exclusively in the Triton X-100 insoluble fraction (Le Fourn et al. 2009). By combined immunoprecipitation–Western blot analysis, we find evidence that deglycosylated EDEM1 in the Triton X-100 insoluble fraction is in complex with p62/SQSTM1 (Fig. 8a, b). In contrast, no evidence was obtained that the Triton X-100 soluble, glycosylated EDEM1 was associated with p62/SQSTM1. p62/SQSTM1 interacts with its ubiquitin-binding domain with ubiquitinated proteins (Bjorkoy et al. 2005; Kirkin et al. 2009; Vadlamudi et al. 1996; Watanabe and Tanaka 2011) to form cytoplasmic p62/SQSTM1 bodies (Johansen and Lamark 2011). In addition, it interacts with LC3-II of autophagy isolation membranes via an LC3-interacting region motif (Ichimura et al. 2008; Kirkin et al. 2009; Pankiv et al. 2007). By combined immunoprecipitation and Western blotting, we found that deglycosylated but not glycosylated EDEM1 was modified by ubiquitin (Fig. 8c). Although not proven, we assume that deglycosylated EDEM1 is polyubiquitinated based on its migration behavior in SDS-PAGE analysis.

Next, we aimed to elucidate the mechanism by which EDEM1 becomes deglycosylated and hypothesized that the cytoplasmic PNGase is involved (Kitajima et al. 1995; Suzuki et al. 1993). To test this, we applied the PNGase inhibitors BODY-$(GlcNAc)_2$-CIAc (Hagihara et al. 2007) and Z-VAD(OMe)-fmk (Misaghi et al. 2004). With both

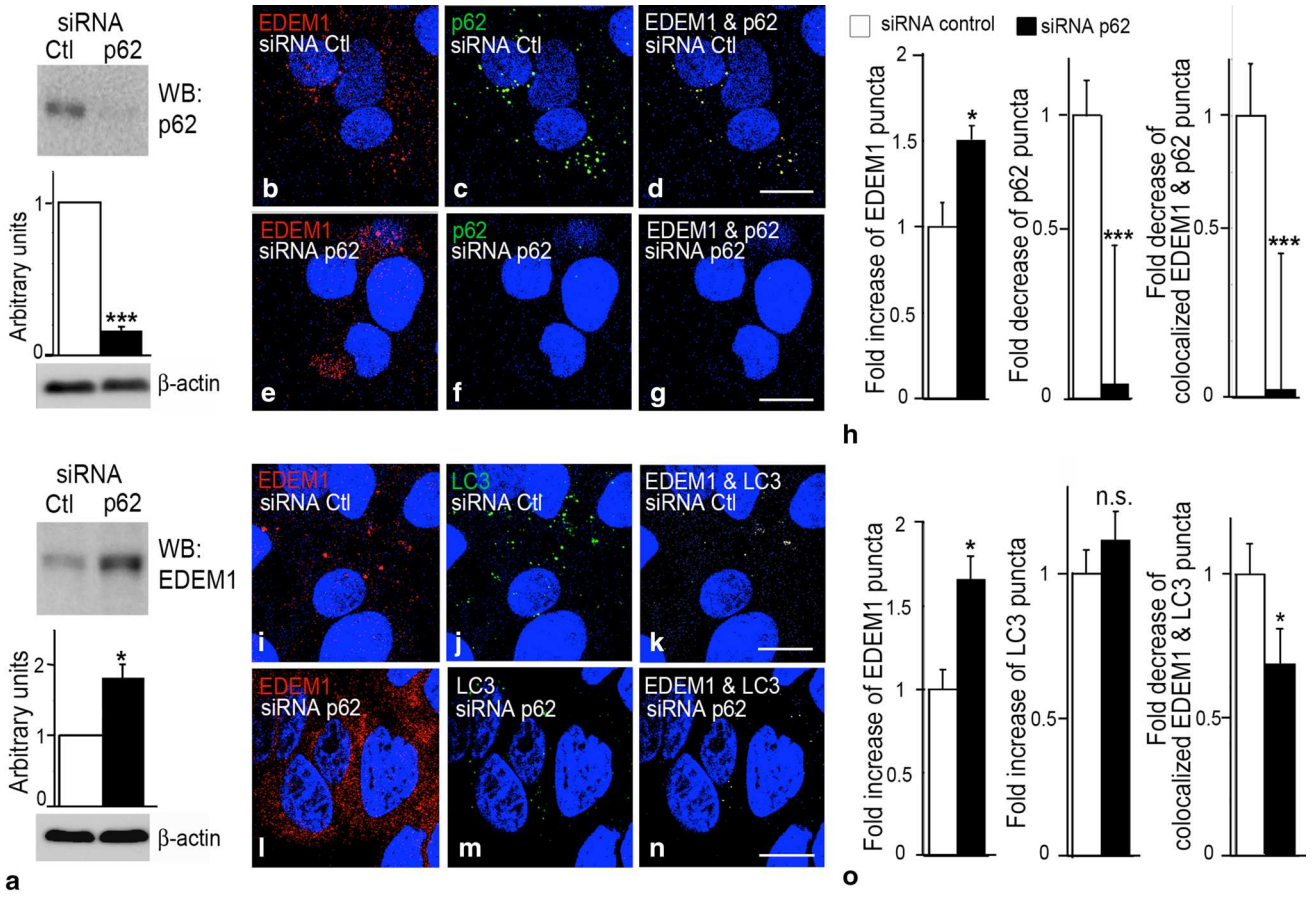

Fig. 6 siRNA silencing of p62/SQSTM1 impedes the colocalization of EDEM1 and LC3. **a** Western blot showing the siRNA knock down of p62/SQSTM1 (*upper panel*) and its effect on EDEM1 protein levels (*lower panel*). **b**–**g** Confocal *top*-to-*bottom* *z*-stacks illustrating the effect of p62/SQSTM1 siRNA knockdown on EDEM1 puncta (**b**, **e**), p62/SQSTM1 puncta (**c**, **f**), and colocalized EDEM1–p62/SQSTM1 puncta (**d**, **g**). *Bars* 10 μm. **h** Quantification of p62/SQSTM1 siRNA knockdown effect on EDEM1 puncta (*left panel*) p62/SQSTM1 puncta (*middle panel*) and their colocalization (*right panel*). **i**–**n** Confocal *top*-to-*bottom* *z*-stacks depicting the effect of p62/SQSTM1 siRNA knockdown on EDEM1 (**i**, **l**) and LC3 (**j**, **m**) puncta and their colocalization (**k**, **n**). *Bars* 10 μm. **o** Quantification of EDEM1 puncta (*left panel*), LC3 puncta (*middle panel*) and colocalized EDEM1 and LC3 puncta (*right panel*) following p62/SQSTM1 siRNA knockdown. $*p < 0.05$; $***p < 0.005$

inhibitors, a significant increase in the amount of glycosylated EDEM1 was observed (Fig. 9a). Since Z-VAD (OMe)-fmk is also a broad-spectrum caspase inhibitor (Garcia-Calvo et al. 1998; Misaghi et al. 2004, 2006), we used the specific inhibitor BODY-$(GlcNAc)_2$-CIAc (Hagihara et al. 2007; Miyazaki et al. 2009) in the further experiments. Strikingly, inhibition of PNGase prevented the wortmannin-induced increase in number and size of EDEM1 puncta (Fig. 9h, k, n, o). However, the number and size of p62/SQSTM1 puncta was not influenced (Fig. 9i, l). Most intriguingly, inhibition of PNGase significantly inhibited the wortmannin-induced colocalization of EDEM1 and p62/SQSTM1 and inhibited the formation of large-size colocalized puncta (Fig. 9j, m, p, q). Together, these results indicate that EDEM1 is a substrate for PNGase and that its deglycosylation by PNGase is required for association with p62/SQSTM1 and subsequent selective autophagy.

Discussion

The ERAD component EDEM1 is a short-lived protein, and its regulated expression in the ER has been shown to be of importance for proper functioning of ERAD (Cali et al. 2008; Le Fourn et al. 2009). A role of basal autophagy in the degradation of EDEM1 was previously documented (Cali et al. 2008; Le Fourn et al. 2009). By combined microscopic and biochemical analysis and Atg siRNA knockdown, endogenous EDEM1 in resting HepG2 cells was unequivocally detected in autophagosomes (Le Fourn et al. 2009). Our present investigation has unraveled novel aspects of the autophagic degradation of EDEM1 (Fig. 10). We show that it exists in the cytoplasm together with the selective cargo receptors p62/SQSTM1, NBR1 and Alfy. Moreover, EDEM1 in complex with p62/SQSTM1, and probably also with NBR1 and Alfy, is deglycosylated

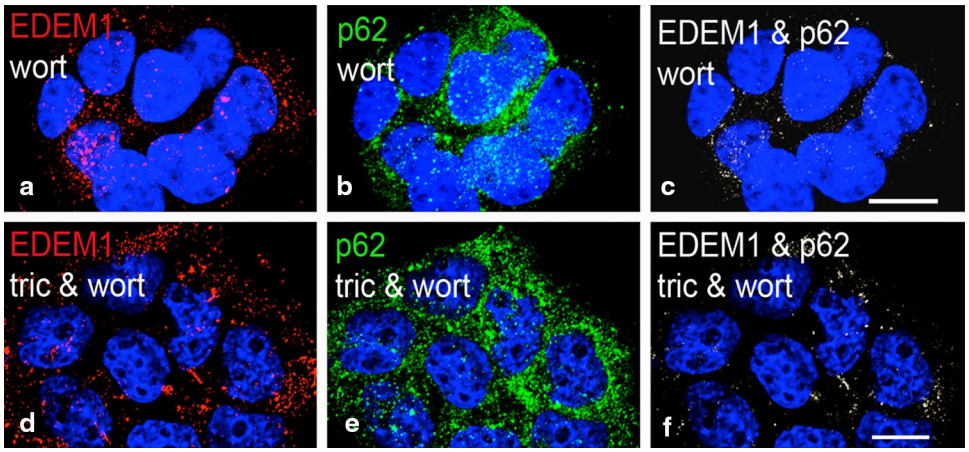

Fig. 7 Aggregation of EDEM1 with p62/SQSTM1 occurs independent of histone deacetylase. **a–c** Confocal *top*-to-*bottom* *z*-stacks illustrating the wortmannin (wort)-induced increased size of EDEM1 puncta (**a**) and p62/SQSTM1 puncta (**b**) and their colocalization (**c**). **d–f** Inhibition of histone deacetylase by trichostatin A (tric) does not prevent wortmannin (wort)-induced formation of large EDEM1–p62/SQSTM1 clusters. *Bars* 10 μm

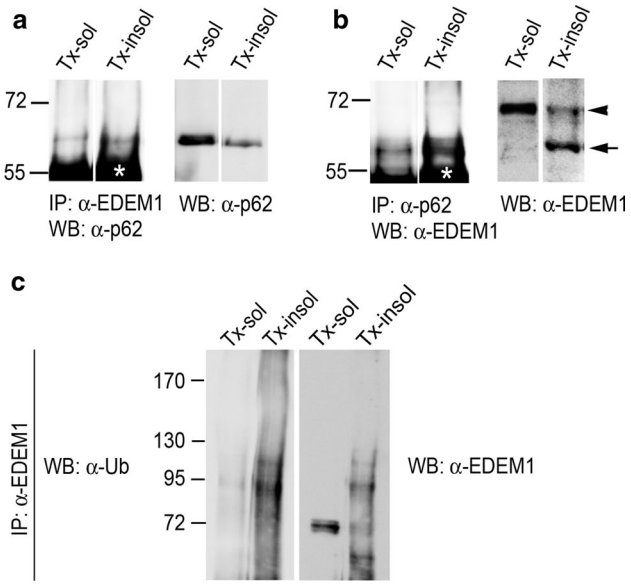

Fig. 8 EDEM1 exists in complex with p62/SQSTM1 and is ubiquitinated. **a**, **b** Combined immunoprecipitation–Western blot analysis of Triton X-100 soluble (Tx-sol) and Triton X-100 insoluble (Tx-insol) fractions shows interaction between p62/SQSTM1 and deglycosylated EDEM1 (*left panels* in **a** and **b**). Western blot of input for p62/SQSTM1 (*right panel* in **a**) and EDEM1 (*right panel* in **b**). *Asterisk* heavy chain of Ig. *Arrowhead* glycosylated EDEM1, *arrow* deglycosylated EDEM1. **c** Combined ubiquitin immunoprecipitation and EDEM1 Western blot analysis indicates ubiquitination of Triton X-100 insoluble EDEM1. Molecular mass is indicated in kilodaltons

and ubiquitinated, and the complexes are detergent-insoluble. By computer prediction (www.ubpred.org), K610 of EDEM1 was scored with high confidence as an ubiquitination site and K616 as well as K116 with medium confidence. We provide evidence that deglycosylation of EDEM1 occurs by the cytosolic PNGase (Park et al. 2001; Suzuki 2007; Suzuki et al. 1993), which appears to be required for its interaction with p62/SQSTM1 and probably the other studied cargo receptors. The interaction with p62/SQSTM1 and NBR1 is a prerequisite for routing of EDEM1 to autophagosomes since it is inhibited by siRNA knockdown of the cargo receptors. Taken together, this indicates that EDEM1 is degraded by selective autophagy. Although it was proposed that EDEM1 vesicles would fuse with endosomes/lysosomes under steady state conditions (Bernasconi et al. 2012), we were unable to detect EDEM1 in endosomes or classical lysosomes by immunogold electron microscopy.

By high-resolution double-label light and electron microscopy, direct evidence could be obtained for the existence of cytoplasmic complexes composed of the selective autophagy cargo receptors NBR1, p62/SQSTM1 as well as Alfy and EDEM1, and this was furthermore confirmed for p62/SQSTM1 and EDEM1 by combined immunoprecipitation and Western blotting. The importance of cargo receptors for autophagy of EDEM1 was demonstrated by siRNA-mediated knockdown. We observed that a reduction in p62/SQSTM1 and NBR1 protein resulted in a significant reduction in colocalized EDEM1 puncta and LC3 puncta. In contrast, siRNA-mediated knockdown of SEL1 had no effect (unpublished data). Together, this indicates that interaction of EDEM1 with p62/SQSTM1 and NBR1 is a prerequisite for its subsequent association with LC3-positive autophagosomal structures. Indeed, by double-immunogold electron microscopy, we observed that clusters of EDEM1 and NBR1, p62/SQSTM1 or Alfy were engulfed by isolation membranes extending our previous findings (Le

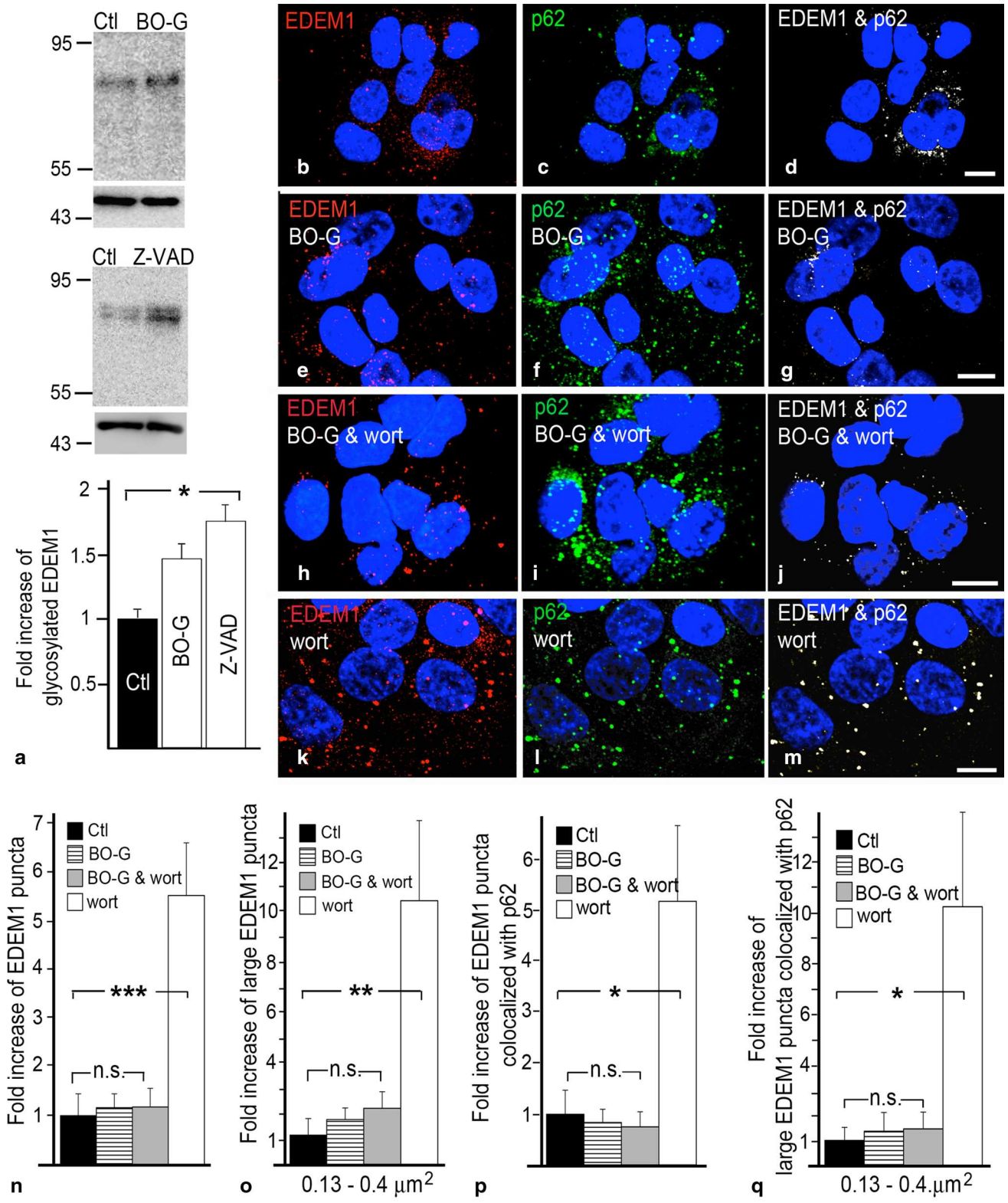

Fig. 9 Deglycosylation of EDEM1 by cytoplasmic PNGase is required for aggregation with p62/SQSTM1. **a** Western blot for EDEM1 of control (Ctl) and PNGase inhibitor-treated (BO-G: BODY-$(GlcNAc)_2$-CIAc for 2 h; Z-VAD: Z-VAD(OMe)-fmk for 3 h) HepG2 cells. The *lower panel* shows the results of quantitative band densitometry. *$p < 0.05$. Confocal *top*-to-*bottom* *z*-stacks show EDEM1 and p62/SQSTM1 and their colocalization in control cells (**b**–**d**), after treatment with PNGase inhibitor BODY-$(GlcNAc)_2$-CIAc (Bo-G) (**e**–**g**), combined PNGase inhibitor and wortmannin treatment (**h**–**j**) and only wortmannin treatment (**k**–**m**). *Bars* 10 µm. Quantification of total (**n**) and large size (0.13–0.4 μm^2) EDEM1 puncta (**o**), and of total (**p**) and large size (0.13–0.4 μm^2) colocalized EDEM1–p62/SQSTM1 puncta (**q**) under control and different experimental conditions. *$p < 0.05$; **$p < 0.01$; ***$p < 0.005$

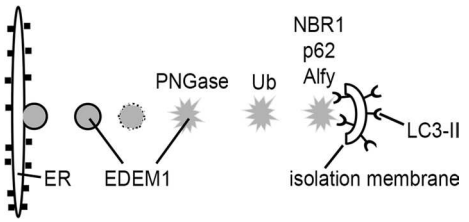

Fig. 10 A schematic presentation summarizing the degradation of EDEM1 by selective autophagy. EDEM1 exits the ER by a vesicular pathway as shown earlier (Zuber et al. 2007). After vesicle membrane dissolution by a not yet defined mechanism, EDEM1 becomes cytoplasmic, is deglycosylated by PNGase and forms detergent-insoluble aggregates. Subsequent to deglycosylation and ubiquitination, interaction with cargo receptors NBR1, p62/SQSTM1 and Alfy occurs that is followed by selective autophagy

Fourn et al. 2009). Complexes of EDEM1 and the cargo receptors are detergent-insoluble and ≥200 nm in size by immunogold labeling. Obviously, aggregates of this size are too large for proteasomal degradation and as demonstrated for other types of cytoplasmic protein aggregates (Bjorkoy et al. 2005; Filimonenko et al. 2010; Metcalf et al. 2012) become degraded by autophagy. Since we have previously shown that EDEM1 exits the ER in non-COPII vesicles (Zuber et al. 2007), it was unanticipated to find it in complex with the cytoplasmic cargo receptors (Johansen and Lamark 2011). Recently, we have made similar observations for the degradation of surplus fibrinogen Aα-γ assembly intermediates in HepG2 cells (Le Fourn et al. 2013). Such fibrinogen assembly intermediates are large, disulfide bridge-linked protein complexes (Mosesson et al. 2001) that cannot be dislocated from the ER lumen to the cytoplasm by the dislocation complex alike small luminal misfolded proteins such as the Hong Kong variant of α1-antitrypsin or misfolded carboxypeptidase Y (Carvalho et al. 2010; Sato et al. 2009). Rather, like EDEM1, they were exported from the ER in vesicles, formed detergent-insoluble aggregates with p62/SQSTM1 and NBR1 and were degraded by selective autophagy (Le Fourn et al. 2013). The present findings imply that the membrane of the EDEM1-containing vesicles becomes permeabilized or dissolved. This seems to involve a specific enzymatic mechanism (manuscript in preparation).

Deglycosylation of EDEM1 and its autophagic degradation are interrelated though the underlying mechanism remained elusive (Le Fourn et al. 2009). Previously, EDEM1 was detected as heterogeneously glycosylated forms and as a single deglycosylated form (Le Fourn et al. 2009). Of note, the deglycosylated EDEM1 existed preferentially as detergent-insoluble aggregates (Le Fourn et al. 2009). Furthermore, glycosylated and deglycosylated EDEM1 were cleared at different rates indicating that deglycosylation occured before degradation (Le Fourn et al. 2009). In fact, only deglycosylated EDEM1 was detected in immunopurified autophagosomes (Le Fourn et al. 2009). As shown here, deglycosylation of EDEM1 occurs by the cytoplasmic PNGase (Suzuki 2007). The importance of the mammalian PNGase in ERAD-mediated protein degradation in yeast and mammalian cells has been recognized for some time. It involves the deglycosylation of misfolded glycoproteins as well as a misfolded ricin toxin A-chain in order that their proteasomal degradation can occur (Hirsch et al. 2003; Joshi et al. 2005; Kim et al. 2006; Suzuki et al. 2001). For this, PNGase acts in complex with Rad23, an ubiquitin-binding protein that escorts proteins to proteasomes (Elsasser and Finley 2005; Madura 2004). Therefore, the PNGase–Rad23 complex links protein deglycosylation with proteasomal degradation (Kim et al. 2006). As we report here, deglycosylated, ubiquitinated EDEM1 is degraded by selective autophagy and not by proteasomes [see also (Le Fourn et al. 2009)]. It remains to be determined whether the cargo receptors form a complex with PNGase of similar function, but different from the "glycoprotein degradation complex" identified for proteasomal degradation of ERAD substrates (Kim et al. 2006; Suzuki 2007). Regardless, our present results add EDEM1 to the limited number of glycoprotein substrates for PNGase (Blom et al. 2004; Kim et al. 2006; Misaghi et al. 2004). Moreover, they suggest an additional function of PNGase in glycoprotein ERAD and selective autophagy in mammalian cells.

In conclusion, our results provide novel insight into the mechanism of the degradation of the ERAD component EDEM1, which occurs by an unanticipated process that leads to its degradation by selective autophagy. Therefore, EDEM1 degradation occurs by a route differing from that followed by ERAD substrates and has parallels with the clearance of cytoplasmic aggregates of misfolded proteins by selective autophagy.

Acknowledgments We would like to thank Jon Soderholm (Yonsei University) for helpful comments on the manuscript. This work was supported by Korean Research WCU Grant R31-10086 (to J. R. and J. W. C.), the National Research Foundation of Korea by the Ministry of Education, Science and Technology (2010-0027736) (to J. R. and J. W. C.) and the Swiss National Science Foundation (to J. R.). Insook Jang is recipient of a fellowship from the Brain Korea 21 program.

References

Araki K, Nagata K (2012) Protein folding and quality control in the ER. In: Morimoto RI, Selkoe DJ, Kelly JW (eds) Protein homeostasis. Cold Spring Harbor Laboratory Press, Cold Spring Harbor, pp 121–145

Bannykh SI, Rowe T, Balch WE (1996) The organization of endoplasmic reticulum export complexes. J Cell Biol 135:19–35

Bernasconi R, Galli C, Noack J, Bianchi S, de Haan C, Reggiori F, Molinari M (2012) Role of the SEL1L: LC3-I complex as

an ERAD tuning receptor in the mammalian ER. Mol Cell 46:809–819
Bhamidipati A, Denic V, Quan EM, Weissman JS (2005) Exploration of the topological requirements of ERAD identifies Yos9p as a lectin sensor of misfolded glycoproteins in the ER lumen. Mol Cell 19:741–751
Bjorkoy G, Lamark T, Brech A, Outzen H, Perander M, Overvatn A, Stenmark H, Johansen T (2005) p62/SQSTM1 forms protein aggregates degraded by autophagy and has a protective effect on huntingtin-induced cell death. J Cell Biol 171:603–614
Blom D, Hirsch C, Stern P, Tortorella D, Ploegh HL (2004) A glycosylated type I membrane protein becomes cytosolic when peptide: N-glycanase is compromised. EMBO J 23:650–658
Braakman I, Bulleid NJ (2011) Protein folding and modification in the mammalian endoplasmic reticulum. Annu Rev Biochem 80:71–99
Buschhorn BA, Kostova Z, Medicherla B, Wolf DH (2004) A genome-wide screen identifies Yos9p as essential for ER-associated degradation of glycoproteins. FEBS Lett 577:422–426
Cali T, Galli C, Olivari S, Molinari M (2008) Segregation and rapid turnover of EDEM1 by an autophagy-like mechanism modulates standard ERAD and folding activities. Biochem Biophys Res Commun 371:405–410
Carvalho P, Stanley AM, Rapoport TA (2010) Retrotranslocation of a misfolded luminal ER protein by the ubiquitin-ligase Hrd1p. Cell 143:579–591
Chen B, Retzlaff M, Roos T, Frydman J (2012) Cellular strategies of protein quality control. In: Morimoto RI, Selkoe DJ, Kelly JW (eds) Protein homeostasis. Cold Spring Harbor Laboratory Press, Cold Spring Harbor, pp 33–46
Clausen TH, Lamark T, Isakson P, Finley K, Larsen KB, Brech A, Overvatn A, Stenmark H, Bjorkoy G, Simonsen A, Johansen T (2010) p62/SQSTM1 and ALFY interact to facilitate the formation of p62 bodies/ALIS and their degradation by autophagy. Autophagy 6:330–344
Clerc S, Hirsch C, Oggier DM, Deprez P, Jakob C, Sommer T, Aebi M (2009) Htm1 protein generates the N-glycan signal for glycoprotein degradation in the endoplasmic reticulum. J Cell Biol 184:159–172
Cormier JH, Tamura T, Sunryd JC, Hebert DN (2009) EDEM1 recognition and delivery of misfolded proteins to the SEL1L-containing ERAD complex. Mol Cell 34:627–633
Denic V, Quan EM, Weissman JS (2006) A luminal surveillance complex that selects misfolded glycoproteins for ER-associated degradation. Cell 126:349–359
Eisele F, Schafer A, Wolf DH (2010) Ubiquitylation in the ERAD pathway. Subcell Biochem 54:136–148
Elsasser S, Finley D (2005) Delivery of ubiquitinated substrates to protein-unfolding machines. Nat Cell Biol 7:742–749
Filimonenko M, Isakson P, Finley KD, Anderson M, Jeong H, Melia TJ, Bartlett BJ, Myers KM, Birkeland HC, Lamark T, Krainc D, Brech A, Stenmark H, Simonsen A, Yamamoto A (2010) The selective macroautophagic degradation of aggregated proteins requires the PI3P-binding protein Alfy. Mol Cell 38:265–279
Furumai R, Komatsu Y, Nishino N, Khochbin S, Yoshida M, Horinouchi S (2001) Potent histone deacetylase inhibitors built from trichostatin A and cyclic tetrapeptide antibiotics including trapoxin. Proc Natl Acad Sci USA 98:87–92
Garcia-Calvo M, Peterson EP, Leiting B, Ruel R, Nicholson DW, Thornberry NA (1998) Inhibition of human caspases by peptide-based and macromolecular inhibitors. J Biol Chem 273:32608–32613
Gauss R, Jarosch E, Sommer T, Hirsch C (2006) A complex of Yos9p and the HRD ligase integrates endoplasmic reticulum quality control into the degradation machinery. Nat Cell Biol 8:849–854
Gauss R, Kanehara K, Carvalho P, Ng DTW, Aebi M (2011) A complex of Pdi1p and the mannosidase Htm1p initiates clearance of unfolded glycoproteins from the endoplasmic reticulum. Mol Cell 42:782–793
Hagihara S, Miyazaki A, Matsuo I, Tatami A, Suzuki T, Ito Y (2007) Fluorescently labeled inhibitor for profiling cytoplasmic peptide: N-glycanase. Glycobiology 17:1070–1076
Helenius A, Aebi M (2004) Roles of N-linked glycans in the endoplasmic reticulum. Annu Rev Biochem 73:1019–1049
Hirano K, Guhl B, Roth J, Ziak M (2009) A cell culture system for the induction of Mallory bodies: Mallory bodies and aggresomes represent different types of inclusion bodies. Histochem Cell Biol 132:293–304
Hirsch C, Blom D, Ploegh HL (2003) A role for N-glycanase in the cytosolic turnover of glycoproteins. EMBO J 22:1036–1046
Hosokawa N, Wada I, Hasegawa K, Yorihuzi T, Tremblay LO, Herscovics A, Nagata K (2001) A novel ER alpha-mannosidase-like protein accelerates ER-associated degradation. EMBO Rep 2:415–422
Hosokawa N, Kamiya Y, Kamiya D, Kato K, Nagata K (2009) Human OS-9, a lectin required for glycoprotein endoplasmic reticulum-associated degradation, recognizes mannose-trimmed N-glycans. J Biol Chem 284:17061–17068
Hosokawa N, Tremblay LO, Sleno B, Kamiya Y, Wada I, Nagata K, Kato K, Herscovics A (2010) EDEM1 accelerates the trimming of a1,2-linked mannose on the C branch of N-glycans. Glycobiology 20:567–575
Hutt DM, Powers ET, Balch WE (2009) The proteostasis boundary in misfolding diseases of membrane traffic. FEBS Lett 583:2639–2646
Ichimura Y, Kumanomidou T, Sou YS, Mizushima T, Ezaki J, Ueno T, Kominami E, Yamane T, Tanaka K, Komatsu M (2008) Structural basis for sorting mechanism of p62 in selective autophagy. J Biol Chem 283:22847–22857
Iwata A, Riley BE, Johnston JA, Kopito RR (2005) HDAC6 and microtubules are required for autophagic degradation of aggregated huntingtin. J Biol Chem 280:40282–40292
Jakob CA, Burda P, Roth J, Aebi M (1998) Degradation of misfolded endoplasmic reticulum glycoproteins in Saccharomyces cerevisiae is determined by a specific oligosaccharide structure. J Cell Biol 142:1223–1233
Jakob CA, Bodmer D, Spirig U, Battig P, Marcil A, Dignard D, Bergeron JJ, Thomas DY, Aebi M (2001) Htm1p, a mannosidase-like protein, is involved in glycoprotein degradation in yeast. EMBO Rep 2:423–430
Johansen T, Lamark T (2011) Selective autophagy mediated by autophagic adapter proteins. Autophagy 7:279–296
Johnston JA, Ward CL, Kopito RR (1998) Aggresomes: a cellular response to misfolded proteins. J Cell Biol 143:1883–1898
Joshi S, Katiyar S, Lennarz WJ (2005) Misfolding of glycoproteins is a prerequisite for peptide: N-glycanase mediated deglycosylation. FEBS Lett 579:823–826
Kabeya Y, Mizushima N, Ueno T, Yamamoto A, Kirisako T, Noda T, Kominami E, Ohsumi Y, Yoshimori T (2000) LC3, a mammalian homologue of yeast Apg8p, is localized in autophagosome membranes after processing. EMBO J 19:5720–5728
Kaganovich D, Kopito R, Frydman J (2008) Misfolded proteins partition between two distinct quality control compartments. Nature 454:1088–1095
Kawaguchi Y, Kovacs JJ, McLaurin A, Vance JM, Ito A, Yao TP (2003) The deacetylase HDAC6 regulates aggresome formation and cell viability in response to misfolded protein stress. Cell 115:727–738
Kim W, Spear ED, Ng DT (2005) Yos9p detects and targets misfolded glycoproteins for ER-associated degradation. Mol Cell 19:753–764
Kim I, Ahn J, Liu C, Tanabe K, Apodaca J, Suzuki T, Rao H (2006) The Png1-Rad23 complex regulates glycoprotein turnover. J Cell Biol 172:211–219

Kirkin V, Lamark T, Sou YS, Bjorkoy G, Nunn JL, Bruun JA, Shvets E, McEwan DG, Clausen TH, Wild P, Bilusic I, Theurillat JP, Overvatn A, Ishii T, Elazar Z, Komatsu M, Dikic I, Johansen T (2009) A role for NBR1 in autophagosomal degradation of ubiquitinated substrates. Mol Cell 33:505–516

Kitajima K, Suzuki T, Kouchi Z, Inoue S, Inoue Y (1995) Identification and distribution of peptide: N-glycanase (PNGase) in mouse organs. Arch Biochem Biophys 319:393–401

Larsen KB, Lamark T, Overvatn A, Harneshaug I, Johansen T, Bjorkoy G (2010) A reporter cell system to monitor autophagy based on p62/SQSTM1. Autophagy 6:784–793

Le Fourn V, Gaplovska-Kysela K, Guhl B, Santimaria R, Zuber C, Roth J (2009) Basal autophagy is involved in the degradation of the ERAD component EDEM1. Cell Mol Life Sci 66:1434–1445

Le Fourn V, Park S, Jang S, Gaplovska-Kysela K, Guhl B, Lee Y, Cho JW, Zuber C, Roth J (2013) Large protein complexes retained in the ER are dislocated by non-COPII vesicles and degraded by selective autophagy. Cell Mol Life Sci 70:1985–2002

Lee JY, Koga H, Kawaguchi Y, Tang W, Wong E, Gao YS, Pandey UB, Kaushik S, Tresse E, Lu J, Taylor JP, Cuervo AM, Yao TP (2010) HDAC6 controls autophagosome maturation essential for ubiquitin-selective quality-control autophagy. EMBO J 29:969–980

Lucocq JM, Brada D, Roth J (1986) Immunolocalization of the oligosaccharide trimming enzyme glucosidase II. J Cell Biol 102:2137–2146

Madura K (2004) Rad23 and Rpn10: perennial wallflowers join the melee. Trends Biochem Sci 29:637–640

Metcalf DJ, Garcia-Arencibia M, Hochfeld WE, Rubinsztein DC (2012) Autophagy and misfolded proteins in neurodegeneration. Exp Neurol 238:22–28

Misaghi S, Pacold ME, Blom D, Ploegh HL, Korbel GA (2004) Using a small molecule inhibitor of peptide: N-glycanase to probe its role in glycoprotein turnover. Chem Biol 11:1677–1687

Misaghi S, Korbel GA, Kessler B, Spooner E, Ploegh HL (2006) z-VAD-fmk inhibits peptide: N-glycanase and may result in ER stress. Cell Death Differ 13:163–165

Miyazaki A, Matsuo I, Hagihara S, Kakegawa A, Suzuki T, Ito Y (2009) Systematic synthesis and inhibitory activity of haloacetamidyl oligosaccharide derivatives toward cytoplasmic peptide: N-glycanase. Glycoconj J 26:133–140

Mizushima N, Komatsu M (2011) Autophagy: renovation of cells and tissues. Cell 147:728–741

Mizushima N, Levine B, Cuervo AM, Klionsky DJ (2008) Autophagy fights disease through cellular self-digestion. Nature 451:1069–1075

Mizushima N, Yoshimori T, Levine B (2010) Methods in mammalian autophagy research. Cell 140:313–326

Mizushima N, Yoshimori T, Ohsumi Y (2011) The role of Atg proteins in autophagosome formation. Annu Rev Cell Dev Biol 27:107–132

Mosesson MW, Siebenlist KR, Meh DA (2001) The structure and biological features of fibrinogen and fibrin. Ann NY Acad Sci 936:11–30

Nakatsukasa K, Nishikawa S, Hosokawa N, Nagata K, Endo T (2001) Mnl1p, an alpha -mannosidase-like protein in yeast Saccharomyces cerevisiae, is required for endoplasmic reticulum-associated degradation of glycoproteins. J Biol Chem 276:8635–8638

Olivari S, Galli C, Alanen H, Ruddock L, Molinari M (2005) A novel stress-induced EDEM variant regulating endoplasmic reticulum-associated glycoprotein degradation. J Biol Chem 280:2424–2428

Olivari S, Cali T, Salo KE, Paganetti P, Ruddock LW, Molinari M (2006) EDEM1 regulates ER-associated degradation by accelerating de-mannosylation of folding-defective polypeptides and by inhibiting their covalent aggregation. Biochem Biophys Res Commun 349:1278–1284

Palade G (1975) Intracellular aspects of the process of protein biosynthesis. Science 189:347–358

Pankiv S, Clausen TH, Lamark T, Brech A, Bruun JA, Outzen H, Overvatn A, Bjorkoy G, Johansen T (2007) p62/SQSTM1 binds directly to Atg8/LC3 to facilitate degradation of ubiquitinated protein aggregates by autophagy. J Biol Chem 282:24131–24145

Pankiv S, Lamark T, Bruun JA, Overvatn A, Bjorkoy G, Johansen T (2010) Nucleocytoplasmic shuttling of p62/SQSTM1 and its role in recruitment of nuclear polyubiquitinated proteins to promyelocytic leukemia bodies. J Biol Chem 285:5941–5953

Park H, Suzuki T, Lennarz WJ (2001) Identification of proteins that interact with mammalian peptide: N-glycanase and implicate this hydrolase in the proteasome-dependent pathway for protein degradation. Proc Natl Acad Sci USA 98:11163–11168

Petiot A, Ogier-Denis E, Blommaart EF, Meijer AJ, Codogno P (2000) Distinct classes of phosphatidylinositol 3′-kinases are involved in signaling pathways that control macroautophagy in HT-29 cells. J Biol Chem 275:992–998

Powis G, Bonjouklian R, Berggren MM, Gallegos A, Abraham R, Ashendel C, Zalkow L, Matter WF, Dodge J, Grindey G et al (1994) Wortmannin, a potent and selective inhibitor of phosphatidylinositol-3-kinase. Cancer Res 54:2419–2423

Quan EM, Kamiya Y, Kamiya D, Denic V, Weibezahn J, Kato K, Weissman JS (2008) Defining the glycan destruction signal for endoplasmic reticulum-associated degradation. Mol Cell 32:870–877

Roth J (1982) The protein A-gold (pAg) technique—a qualitative and quantitative approach for antigen localization on thin sections. In: Bullock G, Petrusz P (eds) Techniques in immunocytochemistry, vol 1. Academic Press, London, pp 108–133

Roth J (1989) Postembedding labeling on Lowicryl K4 M tissue sections: detection and modification of cellular components. In: Tartakoff AM (ed) Methods in cell biology, vol 31. Academic Press, San Diego, pp 513–551

Roth J, Bendayan M, Orci L (1978) Ultrastructural localization of intracellular antigens by the use of protein A-gold complex. J Histochem Cytochem 26:1074–1081

Roth J, Taatjes DJ, Warhol MJ (1989) Prevention of non-specific interactions of gold-labeled reagents on tissue sections. Histochemistry 92:47–56

Roth J, Zuber C, Park S, Jang I, Lee Y, Kysela KG, Le Fourn V, Santimaria R, Guhl B, Cho JW (2010) Protein N-glycosylation, protein folding, and protein quality control. Mol Cells 30:497–506

Sato BK, Schulz D, Do PH, Hampton RY (2009) Misfolded membrane proteins are specifically recognized by the transmembrane domain of the Hrd1p ubiquitin ligase. Mol Cell 34:212–222

Simonsen A, Birkeland HC, Gillooly DJ, Mizushima N, Kuma A, Yoshimori T, Slagsvold T, Brech A, Stenmark H (2004) Alfy, a novel FYVE-domain-containing protein associated with protein granules and autophagic membranes. J Cell Sci 117:4239–4251

Suzuki T (2007) Cytoplasmic peptide: N-glycanase and catabolic pathway for free N-glycans in the cytosol. Semin Cell Dev Biol 18:762–769

Suzuki T, Seko A, Kitajima K, Inoue Y, Inoue S (1993) Identification of peptide: N-glycanase activity in mammalian-derived cultured cells. Biochem Biophys Res Commun 194:1124–1130

Suzuki T, Park H, Kwofie MA, Lennarz WJ (2001) Rad23 provides a link between the Png1 deglycosylating enzyme and the 26 S proteasome in yeast. J Biol Chem 276:21601–21607

Szathmary R, Bielmann R, Nita-Lazar M, Burda P, Jakob CA (2005) Yos9 protein is essential for degradation of misfolded glycoproteins and may function as lectin in ERAD. Mol Cell 19:765–775

Szeto J, Kaniuk NA, Canadien V, Nisman R, Mizushima N, Yoshimori T, Bazett-Jones DP, Brumell JH (2006) ALIS are stress-induced protein storage compartments for substrates of the proteasome and autophagy. Autophagy 2:189–199

Tamura T, Cormier JH, Hebert DN (2011) Characterization of early EDEM1 protein maturation events and their functional implications. J Biol Chem 286:24906–24915

Tokuyasu K (1989) Use of poly(vinylpyrrolidone) and poly(vinyl alcohol) for cryoultramicrotomy. Histochem J 21:163–171

Vadlamudi RK, Joung I, Strominger JL, Shin J (1996) p62, a phosphotyrosine-independent ligand of the SH2 domain of p56lck, belongs to a new class of ubiquitin-binding proteins. J Biol Chem 271:20235–20237

Wang K, Klionsky DJ (2011) Mitochondria removal by autophagy. Autophagy 7:297–300

Watanabe Y, Tanaka M (2011) p62/SQSTM1 in autophagic clearance of a non-ubiquitylated substrate. J Cell Sci 124:2692–2701

Wipf P, Halter RJ (2005) Chemistry and biology of wortmannin. Org Biomol Chem 3:2053–2061

Wolf DH (2011) The ubiquitin clan: a protein family essential for life. FEBS Lett 585:2769–2771

Wong E, Cuervo AM (2012) Integration of clearance mechanisms: the proteasome and autophagy. In: Morimoto RI, Selkoe DJ, Kelly JW (eds) Protein homeostasis. Cold Spring Harbor Laboratory Press, Cold Spring Harbor, pp 47–65

Wu YT, Tan HL, Shui G, Bauvy C, Huang Q, Wenk MR, Ong CN, Codogno P, Shen HM (2010) Dual role of 3-methyladenine in modulation of autophagy via different temporal patterns of inhibition on class I and III phosphoinositide 3-kinase. J Biol Chem 285:10850–10861

Zatloukal K, Stumptner C, Fuchsbichler A, Heid H, Schnoelzer M, Kenner L, Kleinert R, Prinz M, Aguzzi A, Denk H (2002) p62 Is a common component of cytoplasmic inclusions in protein aggregation diseases. Am J Pathol 160:255–263

Zuber C, Roth J (2009) N-Glycosylation. In: Gabius H (ed) The sugar code. Wiley-VCH, Weinheim, pp 87–110

Zuber C, Spiro MJ, Guhl B, Spiro RG, Roth J (2000) Golgi apparatus immunolocalization of endomannosidase suggests post-endoplasmic reticulum glucose trimming: implications for quality control. Mol Biol Cell 11:4227–4240

Zuber C, Fan JY, Guhl B, Parodi A, Fessler JH, Parker C, Roth J (2001) Immunolocalization of UDP-glucose: glycoprotein glucosyltransferase indicates involvement of pre-Golgi intermediates in protein quality control. Proc Natl Acad Sci USA 98:10710–10715

Zuber C, Cormier JH, Guhl B, Santimaria R, Hebert DN, Roth J (2007) EDEM1 reveals a quality control vesicular transport pathway out of the endoplasmic reticulum not involving the COPII exit sites. Proc Natl Acad Sci USA 104:4407–4412